Pregnancy Reduces COVID-19 Vaccine Immunity Against Novel Variants

Maclaine A. Parish[1], Jaiprasath Sachithanandham[1], Lizeth Gutierrez[2], Han-Sol Park[1], Anna Yin[1], Katerina Roznik[2], Patrick Creisher[1], John S. Lee[1], Laura A. St Clair, [1] Annie Werner[1], Catherine Pilgrim-Grayson[4], Lea Berhane[5], Hana Golding[6], Patrick Shea[1], Katherine Fenstermacher[7], Richard Rothman[7], Irina Burd[8], Jeanne Sheffield[9], Andrea L. Cox[1,2], Andrew Pekosz[1,2,7], and Sabra L. Klein[1,2*]

[1]W. Harry Feinstone Department of Molecular Microbiology and Immunology, Johns Hopkins University Bloomberg School of Public Health, Baltimore, MD, USA

[2]Department of Medicine, Division of Infectious Diseases, Johns Hopkins School of Medicine, Baltimore, MD, USA

[4] Division of Rare Diseases and Medical Genetics; Office of Rare Diseases, Pediatrics, Urologic and Reproductive Medicine; Office of New Drugs; Center for Drug Evaluation and Research; U.S. Food and Drug Administration, Silver Spring, MD, USA

[5]Division of Clinical Policy, Office of New Drug Policy, Office of New Drugs; Center for Drug Evaluation and Research; U.S. Food and Drug Administration, Silver Spring, MD, USA

[6]Division of Viral Products, Center of Biologics Evaluation and Research, U.S. Food and Drug Administration, Silver Spring, MD, USA

[7]Department of Emergency Medicine, Johns Hopkins School of Medicine, Baltimore, MD, USA

[8]Department of Obstetrics, Gynecology and Reproductive Sciences, University of Maryland School of Medicine, Baltimore, MD, USA

[9]Department of Obstetrics and Gynecology, Johns Hopkins School of Medicine, Baltimore, MD, USA

*Address correspondence to Sabra L. Klein, (410)955-8898, sklein2@jhu.edu

Abstract

Pregnant women are at heightened risk for severe outcomes from infectious diseases like COVID-19, yet were not included in initial vaccine trials, which may contribute to low booster uptake (15% or lower). We explored the serological and cellular responses to COVID-19 mRNA booster vaccines (i.e., ancestral and BA.5) in pregnant and age-matched, non-pregnant females to identify how pregnancy affects immunity against vaccine and novel variants. Antibodies from pregnant women were less cross-reactive to non-vaccine antigens, including XBB.1.5 and JN.1. Non-pregnant females showed greater IgG1:IgG3 ratios and neutralization against all variants. In contrast, pregnant women had lower IgG1:IgG3 ratios and neutralization but increased antibody-dependent NK cell cytokine production and neutrophil phagocytosis, especially against novel variants. Pregnancy increased memory CD4+ T cells IFNγ production, monofunctional dominance, and fatty acid oxidation. Pregnancy may reduce the breadth, composition, and magnitude of humoral and cellular immunity, particularly in response to novel variants.

40 **Introduction**

41 Pregnant women faced significant morbidity and mortality during the COVID-19
42 pandemic, with an elevated risk for severe outcomes [1-3]. From the onset of the pandemic
43 in early 2020 to December 2022, there were 24,203 cases of COVID-19 among pregnant
44 women in the United States with 2,043 fatalities [4]. This 8.4% mortality rate is significantly
45 higher than that of the general population (0.061%), reflecting the elevated risk for disease
46 outcomes in pregnancy. Pregnant women also were more likely to require hospitalization
47 and invasive ventilation from acute SARS-CoV-2 infection than non-pregnant women [3, 4].
48 Adverse pregnancy and neonatal outcomes were an additional concern, as SARS-CoV-2
49 infection has been associated with preeclampsia, stillbirth, NICU admission, and preterm
50 birth in women [1, 5-9] and mouse models [10].

51 American College of Obstetricians and Gynecologists (ACOG) recommend
52 vaccination during pregnancy to provide optimal protection against SARS-CoV-2 for both
53 the mother and fetus [11]. Data from November 2021 show vaccination rates among
54 pregnant women (45.1%) were significantly lower than that of non-pregnant individuals
55 (64.9%) [12]. Vaccination rates among pregnant women have since fallen precipitously, and
56 remain lower than the general population, with less than 15% of pregnant women
57 vaccinated in the 2023-2024 vaccination season [13]. This decline in vaccine uptake is
58 particularly concerning given that other vaccines offered during pregnancy, such as
59 influenza and Tdap, show higher coverage rates (47.4% and 59.6%, respectively) [14, 15].
60 Despite a favorable benefit of administering COVID-19 vaccines during pregnancy [16-18],
61 low vaccine uptake may be a result of greater vaccine hesitancy in this population [19-24].

62 While vaccination is the best preventative strategy to reduce the severity of COVID-
63 19 outcomes [16, 25], existing evidence suggests pregnant women mount dampened
64 immune responses to vaccination, highlighting the need for deeper immunological
65 assessments [26]. While evidence investigating the immunogenicity of COVID-19 vaccines
66 in pregnant women showed effective neutralizing antibody responses to primary mRNA
67 vaccine two-shot series and efficient maternal antibody transfer via cord blood [27-29],
68 data on cross-protection elicited by vaccination are limited. Previous studies of COVID-19
69 vaccines in pregnant women have focused on placental antibody transfer, demonstrating
70 the benefits of maternal vaccination in protecting newborns and infants from severe
71 infection [30-32]. While several studies have aimed to compare the antibody landscape
72 induced by vaccination during pregnancy with those in non-pregnant women [33], to date,
73 the effects of pregnancy on cross-protection against circulating variants in addition to
74 vaccine antigens have remained unexplored.

75 Using systems serology, we can broadly and deeply characterize the antibody
76 landscape in response to COVID-19 vaccination. By employing this systematic and
77 comprehensive approach, we can gain insight to shape future vaccine development and
78 public-health campaigns by understanding the protective immune response generated by
79 vaccination [34]. Combining functional assays and systems serology methods, we show
80 that the breadth and diversity of antibody generated by vaccination and polyfunctionality of
81 spike-specific memory CD4+ T cells are reduced during pregnancy.

82

83 **Results**

84 ***Pregnancy alters IgG subtype dominance in response to novel variants***

85 Because SARS-CoV-2 nucleocapsid (N) antibodies are not generated by mRNA
86 vaccines targeted to S protein, this can be used as a proxy for SARS-CoV-2 infection [46],
87 with recognized limitations [37]. There was no increase in either anti-N IgG **(Figure 1A)** or in
88 any subclass of IgG1-4 **(Supplemental Figure 1A)** in any participants, suggesting that no
89 one was infected with SARS-CoV-2 during their study enrollment window. However, all
90 participants had detectable anti-N IgG levels highlighting prior exposure to SARS-CoV-2 in
91 our cohort. Luminex-bead assays were used to comprehensively characterize the antibody
92 response generated by vaccination against SARS-CoV-2 vaccine antigens (ancestral and
93 BA.5 S) and circulating variants (XBB.1.5 and JN.1 S). COVID-19 boosters induced IgG in
94 both pregnant and non-pregnant females to circulating variants **(Figure 1B)**. Similar to anti-
95 N IgG, prior to vaccination, total IgG to ancestral S and BA.5 S was high in both cohorts, as
96 SARS-CoV-2 exposure through infection and prior vaccination is pervasive in the general
97 population [47]. This was reflected by limited increase in anti-S IgG responses to vaccine
98 variants (ancestral and BA.5) as pre-existing immunity was high at baseline. In contrast,
99 anti-S IgG increased in response to novel variants (XBB.1.5 and JN.1) likely as a result of
100 lower pre-existing immunity. There were, however, distinct differences in the IgG subtype
101 dominance across groups. When comparing relative isotype abundance, there was IgG1
102 subtype dominance among non-pregnant, but not pregnant, females, particularly in
103 response to JN.1 ($p = 0.04$) **(Figure 1C-F).** While IgG3 contributed to a small proportion of
104 total IgG generated in response to vaccination, pregnant women were more likely to induce
105 anti-S IgG3 than non-pregnant females, particularly against BA.5, while non-pregnant

106 women were more likely to induce IgG4 **(Supplemental Figure 1 B-E).** Non-pregnant
107 women induced anti-S IgG4 responses against all variants. While this is atypical for
108 traditional vaccine responses, evidence in the literature suggest this may be a signature of
109 immune imprinting from subsequent vaccination with mRNA boosters [48]. While not
110 investigated here, it has been suggested that this may be evidence of immune tolerance
111 and may be related to incidence of breakthrough infection [48, 49].

112 ***Pregnancy reduces the cross-neutralizing capacity of antibodies recognizing SARS-***
113 ***CoV-2 variants***

114 The ratio of IgG1:IgG3 has been shown to be predictive of SARS-CoV-2 neutralization
115 capacity [50]. Compared with non-pregnant females, pregnant women had reduced
116 IgG1:IgG3 ratios, particularly to novel variants, (JN.1 $p = 0.02$, XBB.1.5 $p = 0.05$) suggesting
117 that the dominant IgG1 response in non-pregnant females may be indicative of broader
118 cross-neutralization **(Figure 2A-D).** This was reflected by reduced neutralizing antibody
119 (nAb) titers in pregnant compared with non-pregnant women to variants (JN.1 $p = 0.07$,
120 XBB.1.5 $p = 0.03$). Both cohorts showed a rise ($p < 0.001$) in nAb titers to ancestral and BA.5
121 viruses after vaccination and were able to effectively neutralize these viruses **(Figure 2E-F)**.
122 Pregnant women, however, had significantly lower nAb titers than non-pregnant females,
123 with many pregnant women failing to reach the limit of detection **(Figure 2E-H)**. In response
124 to XBB.1.5, while vaccination significantly increased nAb titers in both groups, these
125 responses were significantly higher in non-pregnant than pregnant females, with 43% (3/7)
126 of pregnant women failing to reach detectable nAb titers in comparison to 15% (2/13) of
127 non-pregnant women. Likewise, among non-pregnant females, vaccination boosted nAb

128 titers against JN.1; there was, however, no vaccine-induced increase in nAb titers among
129 pregnant women, with only 28% (2/7) surpassing the limit of detection. **(Figure 2G-H)**. This
130 is further reflected by modest positive correlations between neutralizing antibody titers and
131 IgG1/IgG3 ratios, among non-pregnant women **(Figure 2J-L),** suggesting their increased
132 IgG1/IgG3 ratios may contribute to the increased neutralizing capacity in comparison to
133 pregnant females, even with small sample sizes**.** These data suggest that there is reduced
134 breadth and cross-reactivity to variants after COVID-19 boosting among pregnant
135 compared with non-pregnant females. A reduction in neutralizing antibody titer, potentially
136 facilitated by a shift in isotype dominance may contribute to reduced protection from
137 vaccination during pregnancy.

138 ***Fc receptor binding is not increased in pregnant women against novel variants***

139 While nAb titers are considered a correlate of protection for SARS-CoV-2 infection
140 [51-53], non-neutralizing functions are also important and may contribute to robust
141 protection from severe disease [54]. Data from mouse models suggest FcR-binding and its
142 associated effector functions are necessary for preventing severe COVID-19 disease [55].
143 To further understand the depth and breadth of antibody generated by mRNA boosters in
144 pregnant women, we investigated FcR binding. Antibody Fc binding to FcγRIIA-R, FcγRIIA-
145 H, FcγRIIb, FcγRIIIA-V, FcγRIIIA-F, FcγRIIIB, FcRn, and FcαR was assessed by a multiplexed
146 Luminex bead assay. FcR binding was similarly induced by vaccination in response to
147 ancestral and BA.5 vaccine antigens among both non-pregnant and pregnant females
148 **(Figure 3A-B).** While non-pregnant females showed similar increases in FcR binding to
149 non-vaccine antigens following vaccination, vaccination did not induce robust changes in

150 FcR binding in pregnant women, with increased binding to only 2/6 FcγRs in response to
151 XBB1.5 and 4/6 FcγRs in response to JN.1 (**Figure 3C-D**).

152 ***Non-neutralizing antibody functions and nAb are negatively correlated among***
153 ***pregnant women***

154 To understand how FcR binding contributes to immunity generated by COVID-19
155 vaccination, several non-neutralizing antibody functions were assessed. Non-neutralizing
156 functions aid in the clearance of infected cells through recruitment of effector cells [56].
157 Antibody-dependent complement deposition (ADCD) was analyzed with a multiplexed
158 Luminex bead assay to measure antibody binding to complement protein C3 as a broad
159 indicator of the ability of serum antibody to induce activation of the complement cascade
160 [42]. ADCD was induced by vaccination in both cohorts in response to only XBB.1.5.
161 (**Figure 4A**). ADCD to ancestral and BA.5 S was high in pre-vaccination samples suggesting
162 high preexisting immune responses through complement activation in both cohorts. Non-
163 pregnant females had decreased post vaccination ADCD to JN.1, which was significantly
164 lower than pregnant females which were unchanged by vaccination. These data highlight
165 the differences between variants and how virus evolution may dictate the type and function
166 of antibody generated in response to vaccination. XBB.1.5 and JN.1 are distinct lineages
167 originating from BA.5 that harbor many mutations on the spike protein which can alter the
168 ability of the virus to evade distinct immune functions [57]. While both variants have
169 evolved antibody evasion strategies, these data suggest they may be leveraged through
170 different mechanisms.

171 In pregnancy, macrophage inflammatory protein (MIP)-1β+ NK cells are found at the
172 maternal-fetal interface and are important for successful implantation and placentation
173 [58]. In NK cells, MIP-1β acts as a chemoattractant in response to activation [59]. Antibody-
174 dependent NK-cell cytotoxicity (ADNK) can be measured through MIP-1β production by NK
175 cells [60]. Although neither cohort induced additional MIP-1β secretion against ancestral,
176 BA.5, or XBB.1.5 following vaccination, MIP-1β+ NK cells were uniquely elevated in
177 pregnant women following vaccination when compared with non-pregnant females (**Figure**
178 **4B**). In NK cells, interferon gamma (IFNγ) acts as an antiviral cytokine to promote further
179 accumulation, activation, and cytotoxicity of NK cells [61]. As an additional readout of
180 ADNK, NK cell IFNγ production post-vaccination was elevated in pregnant women in
181 response to BA.5 and in non-pregnant females in response to JN.1 **(Supplemental Figure**
182 **3A).** There were no changes post-vaccination in NK-cell degranulation, as marked by
183 CD107a+ NK cells, among either cohort **(Supplemental Figure 3B)**. While vaccination did
184 not increase ADNK capacity to vaccine antigens in either cohort, elevated ADNK in
185 pregnant women in comparison to non-pregnant women may be important for
186 understanding the antiviral and functional capacity of antibodies generated by vaccination.
187 Antibody-dependent cellular phagocytosis (ADCP) and antibody-dependent
188 neutrophil phagocytosis (ADNP) assess the ability of antibody to induce macrophage and
189 neutrophil phagocytosis of antigen, respectively, and are reported as a PhagoScore [43],
190 representing both the function and number of beads phagocytosed. While inconsistent
191 across variants and groups, ADCP tended to decrease among non-pregnant women while
192 no changes in PhagoScores were observed in pregnant women. ADNP followed a similar

193 trend among non-pregnant women. Among pregnant women, however, ADNP decreased
194 against ancestral and JN.1 antigens while there was no change in response to either BA.5
195 or XBB.1.5 post vaccination (**Figure 4C**). This is likely indicative of shifting dynamics
196 between neutralizing and non-neutralizing functions, a phenomenon that has been
197 documented in the context of repeat vaccination and may be a result of immune imprinting
198 mechanisms [62]. Correlation analyses revealed significant negative correlations between
199 nAb titers and ADNP PhagoScores among pregnant women only, further suggesting a shift
200 away from neutralization, and towards non-neutralizing neutrophil phagocytosis among
201 pregnant women (**Figure 4E-H**). For JN.1, correlation analyses were non-significant likely
202 because responses from many pregnant women were below the limit of detection for nAb
203 titer (**Figure 4H**). In non-pregnant females, while negative correlations between nAb titers
204 and ADNP were seen in response JN.1, ancestral, BA.5 and XBB.1.5, these associations
205 were non-significant, suggesting small sample sizes may preclude strong conclusions.

206 ***Altered correlations among IgG subclasses and antibody functional phenotypes in***
207 ***pregnant women***

208 Correlation matrices can be used to examine complex relationships between
209 antibody isotypes and effector functions assessed by systems serology [63]. These
210 analyses can highlight isotype dependence and may reveal differences in subclass
211 functionality [63]. Spearman correlation matrices were generated to assess correlations
212 between IgG isotypes and FcR binding and antibody functional properties prior to and in
213 response to vaccine and variant viruses (**Figure 5**). Prior to vaccination, there was no IgG
214 subtype dominance, but there were stronger positive associations between IgG subclasses

215 and antibody functional outcomes, including in response to variants (**Figure 5A)**. Matrices
216 of post-vaccination samples were most different between pregnant and non-pregnant
217 women for variants, with fewer strong correlations in pregnant than non-pregnant women.
218 Among non-pregnant women, anti-S IgG1 was positively and anti-S IgG3 was negatively
219 correlated with FcR binding as well as neutralizing and non-neutralizing antibody functions,
220 particularly against variants. This trend was reversed in pregnant women, in which anti-S
221 IgG3 was positively and anti-S IgG1tended to be negatively correlated with Fc receptor
222 binding and functional outputs. These data further implicate the reduced IgG1:IgG3 ratio
223 and isotype subclass switching as functionally altering antibody-mediated immunity in
224 pregnant women.

225 ***Decreased polyfunctional CD4⁺ T cells responses in pregnant women***

226 Because immunoglobulin subtype switching depends on CD4⁺ T-cell help and
227 cytokine production [64], we hypothesized that differences in CD4⁺ T-cell cytokine
228 production between pregnant and nonpregnant females may contribute to differences in
229 isotype switching and IgG subtypes. We assessed intracellular-cytokine production by
230 memory CD4⁺ T cells **(Supplemental Figure 3A)** and CD8⁺ T cells **(Supplemental Figure**
231 **4A)** in pregnant and non-pregnant women in response to ancestral S-peptide pools [65, 66]
232 prior to and after vaccination by measuring IFNγ, TNF, IL-2, and IL-21 secretion
233 **(Supplemental Figures 3B, 4B)**. While individual cytokine frequencies provided initial
234 insight into S-specific CD4⁺ memory T cell responses, comprehensive assessment of T cell
235 functionality requires analysis of polyfunctional responses. Polyfunctionality is defined as
236 the ability for individual cells to produce more than one cytokine simultaneously [67]. This

237 approach is particularly important considering preliminary analysis of limited class-
238 switching in pregnant participants, with polyfunctional $CD4^+$ T-cell responses being known
239 to enhance nAb titers and immunity following vaccination against multiple pathogens,
240 including SARS-CoV-2 [68-70]. To characterize the functionality of $CD4^+$ T cell responses,
241 Boolean gating analysis identified all (15) possible combinations of the four measured
242 cytokines represented as pie charts (**Figure 6A-B**) or histograms (**Supplemental Figure 5**).
243 Intracellular cytokine staining of $CD4^+$ T cells in response to ancestral S-peptide
244 stimulation at post-vaccination timepoints suggested differences in cytokine profiles
245 between groups **(Figure 6).** While both pregnant and non-pregnant women had IFNγ+
246 monofunctional $CD4^+$ T cells, pregnant women tended to have proportionally higher
247 frequencies of these cells. In $CD4^+$ T cells, IFNγ production is known to modulate class
248 switching in B cells, particularly favoring IgG3 over IgG1 [71-73]. Non-pregnant women
249 showed a trend toward greater $CD4^+$ T cell polyfunctionality, with more cells co-expressing
250 multiple cytokines including IL-21, TNF and IL-2 (**Figure 6B**), cytokines that influence B cell
251 maturation and antibody production. IL-2 is essential for T cell proliferation and survival,
252 particularly supporting the development and maintenance of T follicular helper (Tfh) cells
253 for germinal center reactions [74]. TNF contributes to germinal center formation and
254 promotes B cell differentiation and isotype switching [75, 76]. Our analysis revealed that
255 TNF production was enhanced in memory $CD4^+$ T cells from pregnant but not non-pregnant
256 females after vaccination. Alterations in polyfunctionality of T cells, and decreased
257 production of these cytokines may contribute to the diminished cross-neutralizing
258 antibody responses and altered IgG subclass distribution among pregnant women. In

259 contrast, no effects of pregnancy or vaccination were observed in intracellular cytokine
260 responses to S in memory CD8$^+$ T cells (**Supplemental Figure 6**).

261 ***Carnitine palmitoyltransferase 1A (CPT1a) expression is elevated* in *T cells of pregnant***
262 ***women***

263 To further investigate phenotypic differences in T cells from pregnant and non-
264 pregnant women, data generated by UMAP (Uniform Manifold Approximation and
265 Projection) and clustering analysis were analyzed for shifts pre- and post-vaccination in
266 both groups. There were no differences in any markers of activation, exhaustion, and
267 metabolism (**Supplemental Table 1**) pre- or post- vaccination between pregnant and non-
268 pregnant except for carnitine palmitoyl transferase 1 A (CPT1a), the rate limiting enzyme in
269 long chain fatty acid oxidation (FAO) [77]. CPT1a was greater in both CD4$^+$and CD8$^+$ T cells
270 prior to vaccination among pregnant compared with non-pregnant females (**Figure 7A-F**).
271 Quantitative analysis of CPT1a mean fluorescence intensity [78] in memory CD4$^+$ T cells
272 revealed that pregnant females maintained approximately 1.5-fold higher expression
273 (31,646 ±,1,372) compared to non-pregnant females (22,885 ± 1,587) prior to and after
274 vaccination **(Figure 7A-B).** This was also seen in the pre-vaccination timepoint for CD8+
275 memory T cells **(Figure 7D).** This is consistent with prior literature showing that gestational
276 changes increase fatty acid availability to T cells [79]. After vaccination CPT1a was reduced
277 in total and memory CD4$^+$ T cells (**Figure 7C-D**), but not in either total or memory CD8+ T
278 cells (**Figure 7E-F**) among pregnant females. In contrast, CPT1a remained constant after
279 vaccination among non-pregnant females.
280

281 **Discussion**

282 Through broad characterization of the antibody landscape following COVID-19
283 vaccination, pregnancy was associated with reduced cross-reactive antibody responses,
284 reflected in decreased IgG1:IgG3 ratios, nAb titers, and FcR-binding in pregnant compared
285 with non-pregnant women. Previous studies have assessed the antibody profile generated
286 by COVID-19 vaccination during pregnancy [31, 33, 80], with a focus on transplacental
287 antibody transfer and protection of babies and infants from severe disease. One study
288 showed limited cross-recognition in pregnant women to non-vaccine antigens after the first
289 doses of ancestral vaccines, without comparison to non-pregnant controls nor assessment
290 of neutralizing responses [31]. Our data illustrate that pregnancy is associated with
291 reduced breadth and lower nAb responses to variants as compared with non-pregnant
292 controls. Continuing efforts to assess antibody responses to updated vaccines remains
293 critical to understanding cross-protection to variants in circulation.

294 SARS-CoV-2 has continued to rapidly evolve and mutate into new variants to escape
295 adaptive-immune responses [81]. In 2022, Omicron variants became dominant in
296 circulation, largely due to an ability to evade nAb generated by ancestral vaccines and
297 natural infections [82]. New variants with the ability to evade nAb continue to emerge and
298 dominate, with XBB.1.5. appearing in October 2022 and peaking in January of 2023, after
299 the inclusion of BA.5 in bivalent booster vaccines was established [83]. By the time XBB.1.5
300 monovalent boosters were accessible, a new variant, JN.1 caused 60% of global cases [83,
301 84]. A potential limitation of annual vaccines is mismatches between dominant circulating
302 strains and updated booster vaccines because variants continue to emerge between

303 annual vaccines strain updates [85-87]. While mRNA technology has increased the speed
304 in which companies can adapt updated vaccines to emerging variants, development of a
305 new booster vaccine still takes several months [88]. Thus, government officials and
306 researchers must work collaboratively to select strains for booster vaccines that will elicit
307 the greatest breadth of immunity [88]. In our study, almost all women were vaccinated
308 against ancestral and BA.5 (bivalent boosters), while XBB.1.5. was the dominant variant in
309 circulation. Our data suggest that pregnancy may limit cross-protective antibodies.
310 Retrospective chart analysis shows that pregnant women are at an elevated risk for
311 breakthrough infection [89]. Similar risk has been shown for other immunologically unique
312 groups including solid-organ transplant recipients and those with autoimmune disease
313 [89]. Thus, our findings of reduced cross-reactive and cross-neutralizing antibodies may
314 provide insight into the mechanism driving elevated risk for breakthrough infection among
315 vulnerable populations.

316 With repeated exposure to antigen through natural infection and booster vaccines,
317 antibody responses to COVID-19 vaccines have evolved and correlates of protection have
318 changed. Total IgG and nAb titers are considered adequate correlates of protection against
319 COVID-19, similar to other acute respiratory infectious diseases [90]. Recent data have
320 suggested that to mount sufficient protection, antibodies against SARS-CoV-2 must
321 possess both neutralizing and non-neutralizing functions as correlates of protection [91].
322 As nAb titers wane and symptomatic cases rise, hospitalization rates among the general
323 population remain low [92]. This provides evidence that other antibody characteristics may
324 be important for protection from severe disease. Our data demonstrate that pregnant

325 women have reduced FcR binding and nAb responses combined with elevated ADNK,
326 especially to non-vaccine antigens.

327 Pregnancy is known to alter antibody glycosylation patterns which can dramatically
328 affect their ability to efficiently and effectively interact with Fc receptors [93, 94]. Structural
329 changes to the antibody-receptor interaction during pregnancy drives nuanced functional
330 consequences that alter cross-reactivity and potentially cross-protection, generated in
331 response to vaccination [93, 94]. In the context of SARS-CoV-2, non-neutralizing antibodies
332 capable of inducing NK cell cytotoxicity were preferentially transferred across the placenta
333 rather than nAb and was driven by differences in antibody glycosylation patterns [95].
334 Future work characterizing antibody glycosylation patterns in pregnant and non-pregnant
335 women could shed light on the mechanisms by which pregnancy alters cross-reactive
336 antibody responses.

337 Our data suggest that reduced class switching and T-cell polyfunctionality may
338 contribute to limited cross-reactivity of antibodies during pregnancy. $CD4^+$ T cells are
339 critical for generation of high affinity, class switched antibodies and contribute to vaccine-
340 induced protection against COVID-19 [96]. Expansion of IFNγ+ monofunctional $CD4^+$ T
341 cells may contribute to reduced IgG1:IgG3 ratios among pregnant women, as these cells
342 may promote IgG3 bias in B cells [71-73]. The observation of a pregnancy-associated
343 metabolic shift toward enhanced FAO compared to non-pregnant participants may reflect
344 a complex dynamic of baseline metabolic reprogramming during pregnancy that may alter
345 vaccination-induced immune responses. Maternal circulation provides a fatty acid-rich
346 environment during the third trimester [79]. The increased expression of CPT1a supports

347 the ability of T cells to use FAO as an energy source in pregnancy. FAO influences the
348 differentiation of $CD4^+$ T cells into different subsets, but the impact of increased FAO on
349 polyfunctionality is not well understood [97, 98]. The small sample sizes in our T cell
350 analyses (N=3 non-pregnant, N=7 pregnant) limit the generalizability of our findings and
351 statistical power to detect meaningful differences. However, despite these small numbers,
352 a statistically significant increase in T cell CPT1a expression provides additional insights
353 into the impact of a fatty acid rich environment in pregnancy. Additional investigation into
354 how this may impact $CD4^+$ T cell polyfunctionality could provide mechanistic insights into
355 pregnancy-associated immune adaptations and highlight the importance of larger studies
356 to confirm these preliminary observations and establish clinical significance to better
357 inform vaccine adherence in the context of pregnancy.

358 While not studied here, maternal antibody transfer is a critical aspect of vaccination
359 during pregnancy, and our data may have implications in our understanding of the
360 protection provided to neonates via cord blood. In fact, a study assessing newborn
361 antibody found that the total number of maternal vaccines received in addition to the
362 timing of the most recent vaccination was a strong predictor of nAb in neonates [99].
363 However, data on the cross-reactivity and cross-protection of these maternally transferred
364 antibodies is lacking. Data from pregnant women and their neonates receiving the primary
365 vaccination series suggest limited Omicron specific IgG and FcR binding [31]. This suggests
366 our data may translate to reduced neonatal protection from maternal antibody transfer.

367 Prior immunization and infection history is an important contributor to immune
368 responses following vaccination and was not analyzed here due to low sample size. In our

369 cohort, there was large amounts of pre-existing immunity reflected by high pre-vaccination
370 levels to a variety of measures including total IgG. Unfortunately, we were unable to directly
371 assess the impact of prior exposures as vaccination and infection records were not
372 available for either cohort of participants. As such it is important to consider the role of
373 immune imprinting when considering cross-reactive and cross-protective antibodies
374 generated through vaccination as immune history may direct the breadth and depth of
375 antibody responses [62]. From data in non-pregnant individuals, immune imprinting is
376 shown to significantly limit the ability of B cells to generate antibody responses to vaccine
377 variants following primary vaccination series [100]. This is an important consideration,
378 particularly as our data suggest pregnancy limits the cross-reactive antibody response and
379 may be further influenced by immune imprinting mechanisms.

380 Although participants in the pregnant and non-pregnant cohorts were age-matched,
381 small sample size limited our ability to consider other demographic variables and impacts
382 the generalizability of our findings. For example, previous studies have shown the impact of
383 trimester on immune responses generated by COVID-19 vaccination [16, 101]. In the
384 present study, sample size limited our ability to assess trimester differences, with 6/7
385 pregnant females enrolled in our study being vaccinated in the second trimester of
386 pregnancy. Additionally, while race is an important consideration to understand differences
387 in immune responses to vaccination, small sample size has limited our ability to stratify
388 data in this way. Consideration of these demographic factors, among others is important
389 and should be a focus of future studies. The small sample size is a major limitation of this
390 study and was associated with challenges recruiting pregnant women. While 232 pregnant

391 women were approached during the study enrollment window, only 7 completed the study.
392 This likely reflects the limited COVID-19 vaccine uptake among pregnant women, which we
393 show is caused by numerous factors across the care continuum that contribute to COVID-
394 19 vaccine hesitancy in this population. Identification of points of public-health
395 intervention to effectively increase vaccine uptake among pregnant women is needed.
396

397 **Methods**

398 ***Study Design***

399 Pregnant women were enrolled into mRNA vaccine studies at the Johns Hopkins Maternal
400 & Fetal Medicine Clinic (IRB 00246472) (n=7 pregnant) during the 2022-2023 vaccination
401 season. Pregnant women were contacted at clinical visits or via phone to determine
402 interest and eligibility. Women were eligible if they planned to receive an mRNA COVID
403 booster vaccine (Pfizer of Moderna) during weeks 32 through 36 of pregnancy, and consent
404 to maternal blood collection before and after receipt of the booster vaccine. Patients who
405 had already received an initial dose(s) of the vaccine were still eligible to enroll.
406 Participants were made aware of the study scope and the anonymity and confidentiality of
407 their collected data. The voluntary nature of their participation, and the details of the study
408 protocol were made evident. All participants gave informed consent to participate in the
409 study. Throughout recruitment, 232 pregnant women were approached to participate in this
410 study. Ninety-one patients were initially interested while only 14 enrolled in the study. Of
411 these, 7 completed the study. Of these seven, two women (distinguished by triangles in all
412 graphs) received monovalent ancestral boosters while the remaining five were recruited

413 after the release of the bivalent ancestral BA.5 booster in August of 2023 and thus received
414 this updated vaccine. For non-pregnant female comparators, samples were obtained from
415 age-matched adult female healthcare workers who were recruited during the 2022-2023
416 influenza vaccine enrollment period by fliers, emails, and announcements about the
417 annual vaccination program and were able to self-enroll upon receipt of the influenza
418 vaccine at the Johns Hopkins East Baltimore hospital (IRB00288258) (n = 13 non-pregnant).
419 All non-pregnant comparators selected as controls for this study received the bivalent
420 ancestral BA.5 booster vaccine. While we have documentation on the vaccine type
421 received at enrollment, prior vaccination and infection records were not available for
422 pregnant nor non-pregnant participants. Demographic information is detailed in **Table 1**. Of
423 the vaccinees enrolled, 13 age-matched non-pregnant females received the COVID-19
424 booster vaccine during the same vaccination season and had pre- and post-vaccination
425 blood samples available. Plasma and peripheral blood mononuclear cells were obtained
426 prior to and one month after receipt of mRNA booster vaccines from pregnant and non-
427 pregnant females. Plasma was used to assess antigen-specific immunoglobulin isotype
428 responses and neutralizing antibody responses, in addition to the crystallizable fragment
429 (Fc) receptor binding and non-neutralizing antibody functions. Cryopreserved PBMCs were
430 used for flow-cytometry analyses.

431 ***Cells and Viruses***

432 VeroE6-TMPRSS2 cells were obtained from the cell repository of the National
433 Institute of Infectious Diseases, Japan, and were grown in complete medium consisting of
434 Dulbecco's modified Eagle's medium (DMEM) (Gibco, Thermo Fisher Scientific),

435 containing 10% fetal bovine serum (FBS) (Gibco, Thermo Fisher Scientific), 1 mM glutamine
436 (Invitrogen, Thermo Fisher Scientific), 1 mM sodium pyruvate (Invitrogen, Thermo Fisher
437 Scientific), 100 U/mL penicillin (Invitrogen, Thermo Fisher Scientific), and 100 µg/mL
438 streptomycin (Invitrogen, Thermo Fisher Scientific). Cells were incubated at 37°C in a
439 humidified incubator with 5% CO_2.

440 Ancestral (hCoV-19/USA/DC-HP00007/2020; B.1, GISAID EPI_ISL_434688), BA.5
441 (hCoV-19/USA/MD-HP32103-PIDCNSQVGY/2022, GISAID EPI_ISL_15013106), XBB.1.5
442 (hCoV-19/USA/MD-HP40900-PIDYSWHNUB/2022, GISAID EPI_ISL_16026423), and JN.1
443 (hCoV-19/USA/MD-HP49672-PIDDVSVURS/2023, GISAID EPI_ISL_18623285) variants of
444 SARS-CoV-2 were isolated in VeroE6-TMPRSS2 cells plated in 24-well plates as previously
445 described [35]. The consensus sequence of the virus isolate did not differ from the
446 sequence derived from the clinical specimen. The infectious virus titer was determined on
447 Vero-E6-TMPRSS2 cells using a 50% tissue culture infectious dose (TCID50) assay as
448 described [36].

449 ***Microneutralization assays***

450 Plasma neutralizing antibodies [37] were determined as described for SARS-CoV
451 and modified for SARS-CoV-2 as described [38]. Two-fold dilutions of plasma, starting at a
452 1:20 dilution, were made using incomplete medium (IM) - Dulbecco's modified Eagle's
453 medium (DMEM) (Gibco, Thermo Fisher Scientific), containing 1 mM glutamine (Invitrogen,
454 Thermo Fisher Scientific), 1 mM sodium pyruvate (Invitrogen, Thermo Fisher Scientific), 100
455 U/mL penicillin (Invitrogen, Thermo Fisher Scientific), and 100 µg/mL streptomycin
456 (Invitrogen, Thermo Fisher Scientific). Infectious virus was added to the plasma dilutions at

457 a final concentration of 1 × 10^3 TCID50/mL or 100 TCID50 per 100 µL. The plasma-virus
458 solution was incubated at room temperature for 1 hour, and 100 µL of each dilution was
459 added to 1 well of a 96-well plate of VeroE6-TMPRSS2 cells in hextuplicate. The cells were
460 incubated for 6 hours at 37°C with 5% CO_2. The inoculum was replaced with fresh IM, and
461 the cells were incubated at 37°C with 5% CO_2 for 3-4 days until cytopathic effect (CPE) is
462 evident in the no serum controls. The cells were fixed by the addition of 100 µL of 4%
463 formaldehyde for at least 4 hours at room temperature and then stained with naphthol
464 blue-black overnight. The nAb titer was calculated as the highest serum dilution that
465 eliminated the CPE in 50% of the wells (NT50), and the AUC was calculated [39, 40].

466 ***Antigen-bead coupling***

467 Antigen-specific isotyping and Fc-receptor binding were multiplexed using a
468 Luminex Intelliflex in a 384-well format. Antigens used in this panel are as follows:
469 ancestral spike (S) and nucleocapsid (N) protein, BA.5, XBB.1.5, and JN.1 spike proteins.
470 These were obtained through the National Cancer Institute Serological Sciences Networks
471 (SeroNet) for COVID-19 [41]. Each antigen was coupled to unique MagPlex bead regions
472 (Luminex). Briefly, beads were activated by combining activation buffer (0.1M NaH2PO4;
473 pH 6.2), 50mg/mL 1-ethyl-3-[3-dimethylaminopropyl] carbodiimide (EDC), and 50mg/mL
474 Sulfo-NHS (N-hydroxysulfosuccinimide). Activated beads were coupled to 25µg of antigen
475 in coupling buffer (0.05M MES; pH 5.0). Activated coupled beads were blocked with
476 blocking buffer (PBS 1X, 0.1% BSA, 0.02% Tween-20, 0.05% sodium azide; pH 7.4), washed
477 with washing buffer (PBS 1X, 0.05% Tween-20) and stored at 4°C in PBS.

478 ***Luminex serological assays***

479 Serum was diluted 1:25 and was incubated with bead solution (20 µL of each bead
480 region in 20 mL of Luminex Assay Buffer: PBS 1X, 0.1% BSA, 0.05% Tween-20). This
481 protocol was followed for isotyping (IgM, IgG [IgG1-4], and IgA [IgA1-2]) and binding to the
482 following Fc receptors (FcRs): FcγRIIA-R, FcγRIIA-H, FcγRIIb, FcγRIIIA-V, FcγRIIIA-F,
483 FcγRIIIB, FcRn, and FcαR (Duke Vaccine Institute – Protein Production facility). Following
484 incubation, plates were placed on a magnet and washed with Procartaplex Wash Buffer
485 (ThermoFisher). Each assay plate was then incubated with 45 µL of secondary antibody
486 diluted in Luminex Assay Buffer. Isotypes were identified by PE-conjugated antibodies
487 (Southern Biotech) and FcR proteins were biotinylated using BirA biotin-ligation kit (Avidity)
488 at least one day prior and coupled to PE-Streptavidin (BioLegend) for 15 min on a rotor
489 before use. Following incubation with secondary antibody, plates were placed on a magnet
490 and washed. Beads were resuspended in Procartaplex Wash Buffer before running on the
491 Luminex Intelliflex. Samples were run on FlexMap 3D Low with a DD range of 7000-1700.
492 For each assay, a minimum of 100 events was recorded per antigen and the MFI of
493 secondary antibody-conjugated to PE, or FcR protein-conjugated to PE for each bead
494 region was measured to quantify antigen-specific immunoglobulin isotypes and FcR
495 responses in each sample at 0- and 28-days post vaccination [42]. LOB (limit of
496 background) for these assays was set by PBS and IgG depleted sera as a negative control.
497 Additional positive controls were included to ensure assay integrity. Optimal serum dilution
498 was determined by a dilution curve to ensure all values fell within the limit of detection.

499 ***Antibody-dependent complement deposition (ADCD)***

500 Serum (1:15 dilution) was added to MagPlex antigen coated beads. Plates were
501 incubated, placed on a magnet, and washed 3 times with 1% BSA. Lyophilized Low-Tox
502 Guinea Pig Complement (Cedarlane) was reconstituted in ice-cold dH2O and diluted 1:25
503 in Gelatin Veronal buffer with Mg^{2+} & Ca^{2+} (GVB++) (Boston Bio). Diluted complement
504 protein was added to each well followed by incubation at 37C. IgG goat anti-guinea pig C3
505 (MP Biomedicals) was diluted 1:500 in 0.1% BSA and added to each well. After incubation,
506 Donkey-anti goat IgG secondary antibody-PE (ThermoFisher) was diluted 1:200 in 0.1% BSA
507 and added to each well. Beads were resuspended in 0.1% BSA and run on the Luminex
508 Intelliflex and data was collected as described above.

509 ***Antibody-dependent NK-cell cytotoxicity (ADNK)***

510 Natural killer (NK) cells were isolated from donor blood. Whole blood was
511 centrifuged through a Ficoll gradient to harvest PBMCs and NK cells were isolated from
512 PBMCs using the MagniSort™ Human NK-cell Enrichment Kit (ThermoFisher). Cell
513 concentration was normalized to 1.5 x 10^6 cells/mL in R10 medium, and IL-15 (1 ng/mL,
514 Abcam) was added and incubated overnight at 37°C. Plates were coated with 3 mg/mL
515 antigen (ancestral, BA.5, XBB.1.5, and JN.1 spike proteins – SeroNet), blocked with 5%
516 BSA, washed, and dried before adding serum (1:100 dilution). Inhibitor cocktail (2.5 µL
517 CD107a-PeCy5 (BD Bioscience - BDB555802) + 0.5 mL BFA (Millipore Sigma) + 1 µL Golgi
518 Stop (BD Bioscience) + 9 mL R10 medium) was added to each well, incubated, and surface
519 staining cocktail (1 µL CD3-Pacific Blue (BD Bioscience - BDB558117) + 1mL CD56-PE-Cy7
520 (BD Bioscience - BDB557747) + 1 mL CD16-APC-Cy7 (BD Bioscience - BDB557758) + 7 mL
521 PBS) is added to a V-bottom 96-well plate. NK cells were transferred to the V-bottom 96

522 well plate with pre-added surface stain cocktail and incubated. Cells were pelleted,
523 supernatant removed, and Perm A (ThermoFisher) was added to each well. Cells were
524 washed and Intracellular staining cocktail (1 mL IFNγ-APC (BD Bioscience -) + 1 mL MIP1-
525 B-PE (BD Bioscience -BDB550078) + 48 mL Perm B (ThermoFisher) was added to each
526 well. Plates were washed, cells were resuspended in PBS and run on a Symphony A3
527 through the Bloomberg Flow Cytometry and Immunology Core. Gating strategy as follows:
528 NK cells- CD3-, CD16+, CD56+ with reported cell populations including IFNγ+, CD107a+
529 and MIP-1β + NK cells.

530 ***Antibody-dependent neutrophil phagocytosis (ADNP)***

531 Antigens (ancestral, BA.5, XBB.1.5, and JN.1 spike proteins – SeroNet) were
532 biotinylated with the BirA biotin-ligation kit (Avidity) and coupled to FluoSpheres™
533 NeutrAvidin™-Labeled Microspheres, 1.0 µm, yellow-green fluorescent (505/515)
534 (ThermoFisher). Antigen was combined with NeutrAvidin beads and incubated. Serum was
535 diluted 1:100 in PBS and incubated with antigen coated beads. During incubation, cells
536 were isolated from donor blood. Whole blood was collected into CPT tubes and centrifuged
537 at 1000 rpm for 30 min. Granulocytes were collected from below the density gradient. Cells
538 were suspended 1:10 in ACK Lysis buffer and incubated at RT for 5 min to lyse red blood
539 cells. Cells were washed and resuspended in 10 mL of PBS. Plates were washed with PBS,
540 200µL of neutrophil solution (5 x 10^6 cells/plate) was added to each well, incubated, spun
541 at 500g for 5 min, and cells were resuspended in extracellular staining solution (0.5µL APC
542 CD66b (BioLegend - 305117) + 19.5mL PBS / well) and incubated for 15min covered with
543 foil at RT. After staining, plates were washed and resuspended in 4% PFA to fix cells,

544 washed and resuspended in PBS. Plates were run on the Attune NxT flow cytometer. Gating
545 on CD66b+ cells (neutrophils) followed by bead+ neutrophils, stained with APC. Data are
546 reported as a PhagoScore, calculated as (% bead-positive neutrophils) * (geometric MFI of
547 each cell) [43].

548 ***Antibody-dependent cellular phagocytosis (ADCP)***

549 THP-1 cells, a human monocytic cell line, were grown in suspension and diluted
550 with warm R10 medium. Following immune complex formation, assay plates are washed
551 with PBS and centrifuged at 2000g for 10 min. The THP-1 cells were plated 2.5 x 10^4 per
552 well, and incubated O/N at 37°C. THP-1 cells were fixed, washed, and resuspended in PBS.
553 Plates are run on the Attune NxT flow cytometer. Gating included bead+ single-cells
554 stained with APC, representing THP-1 cells that have phagocytosed bead. Data are
555 reported as a PhagoScore, calculated as (% bead-positive THP-1) * (geometric MFI of each
556 cell) [44].

557 ***Ex vivo flow cytometry staining***

558 Intracellular cytokine-flow cytometry staining was used to assess antigen-specific
559 cytokine production and T-cell phenotypic and functional profiles. Cryopreserved PBMCs
560 were thawed, rested, and cultured overnight with 1 mg/mL peptide pools consisting of 315
561 peptides (15-mers with 11 amino acid overlap) spanning the ancestral SARS-CoV-2 spike
562 protein (JPT Peptide Technologies, PM-WCPV-S-1) or a DMSO (unstimulated) control. After
563 overnight incubation, cells were washed and stained for viability with Invitrogen Live/Dead
564 Fixable Blue Dead Cell Stain (L34962) and Fc Block (564219). Cell-surface staining was
565 performed with our T-cell panel surface-antibody cocktail mix (**Supplementary Methods**

566 **Table 1A).** Cells were fixed and permeabilized with a 1X Fixation/Permeabilization buffer
567 from eBioscience (FoxP3/Transcription Factor Staining Buffer Set). Intracellular staining
568 was performed with intracellular cytokine-antibody cocktail mix (**Supplementary Methods**
569 **Table 1B**). Cells were resuspended in 1% paraformaldehyde and run on the 4-laser (16UV-
570 16V-15B-8R) Cytek Biosciences Aurora spectral flow cytometer. For ICS, data were
571 processed using biexponential transformation and exported for further analysis in FlowJo to
572 assess cytokine-producing, antigen-specific T cells (**Supplemental Figure 3-4**).
573 Polyfunctionality of these T cells was analyzed with Pestle v2.0 and SPICE 6 v6.1.
574 Metabolic, activation, and exhaustions markers were analyzed via Uniform Manifold
575 Approximation and Projection (UMAP) (v4.1.1), Xshift (v1.4.1), and ClusterExplorer (v1.7.6).

576 ***Statistical analyses***

577 GraphPad Prism v10.1 was used to perform univariate analyses with details about
578 statistical tests used for each dataset described in further detail in figure legends.
579 Spearman correlations of systems serology measures were visualized in heatmaps
580 generated using R v4.2.3 and version 1.0.12 of the package "pheatmap" (https://cran.r-
581 project.org/web/packages/pheatmap [45]. For ADNP and ADNK assays, data were
582 averaged across two healthy donors. Flow FCS files were analyzed using FlowJo v10
583 (10.8.1) software. Gating strategy for ICS can be found in **Supplementary Figures 3** and **4**.
584 ICS data were exported from Pestle v2.0 and SPICE 6 v6.1 for further statistical analyses
585 detailed in figure legends.

586

587 **Data Availability**

588 All anonymized data that support the findings of this study can be made available upon
589 request from the corresponding author.
590

591 **Acknowledgements.** We thank the clinical coordinators and vaccinees for making this
592 study possible. We are especially grateful to Kimberly Jones-Beatty and Michelle Ufua for
593 their assistance with recruitment. Thank you to Galit Alter, Ryan McNamara, and Taras
594 Chicz for graciously training lab members and sharing protocols to develop systems
595 serology methods. We thank Prakash Srinivasan for the use of the Attune Nxt flow
596 cytometer and the Bloomberg Flow Cytometry and Immunology Core. This study was
597 supported by the Food and Drug Administration (FDA) of the U.S. Department of Health and
598 Human Services (HHS) as part of a financial assistance award [Center of Excellence in
599 Regulatory Science and Innovation grant to Johns Hopkins University, U01FD005946]
600 totaling $415,256 with 75% percentage funded by FDA/ OWH. The contents are those of the
601 author(s) and do not necessarily represent the official views of, nor an endorsement, by
602 FDA/OWH, or the U.S. Government. FDA CERSI U01FD005942 (SLK), NIH NIAID
603 75N93021C00045 (AP, RR), NIH NCI U54 CA260492 (SLK, ALC).
604

605 **Author Contributions**

606 SLK, IB, AP, and ALC conceptualized the experimental design and group comparisons for
607 this study. MAP, H-SP, JSL, LStC, PS, IB, JS, KF, RR, and ALC identified, acquired, stored, and
608 distributed patient samples and clinical and demographic data for analyses. MAP, H-SP,
609 PC, AW and JSL developed and validated serological assays. MAP, JS, LG and H-SP

processed samples and completed technical assays. MAP, KR, and AY conducted statistical analyses. MAP, LG, KR, ALC, and SLK developed all tables and figures. MAP, ALC, SLK wrote the initial draft of the manuscript. MAP, JS, LG, HSP, AY, KR, PC, JSL, LAS, AW, CPG, LB, HG, PS, KF, RR, IB, JS, ALC, AP, and SLC provided substantive edits and approved the final draft of the manuscript.

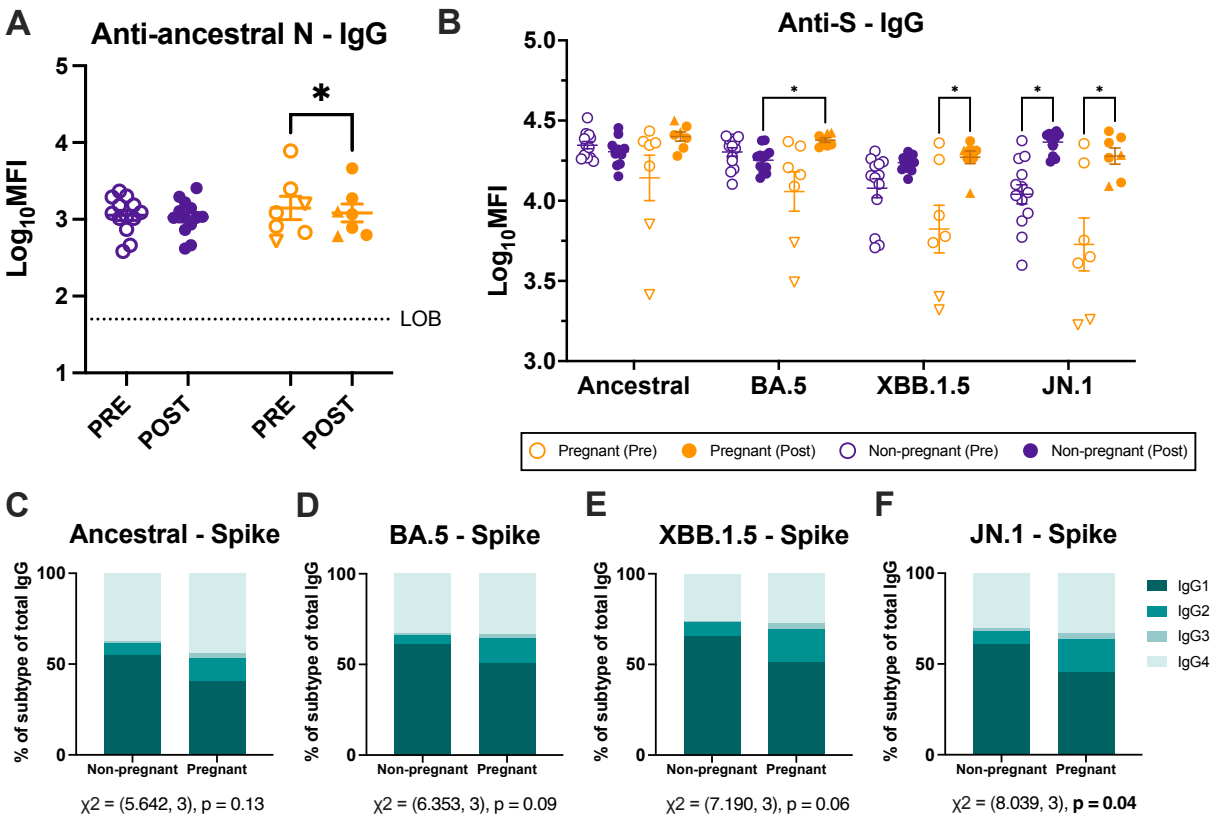

Figure 1. Vaccination differently induces IgG subtype responses during pregnancy. IgG antibody responses in serum pre and 3-5 weeks post-vaccination were measured by systems serology and reported as $\log_{10}$ mean fluorescence intensity. Pregnant women (n=7) are shown in orange and non-pregnant females (n=13) in purple. Triangles highlight women who received monovalent boosters and circles represent bivalent booster recipients. Horizontal bars indicate mean MFI across samples with bars indicating standard error of the mean. **(A)** Total IgG to ancestral nucleocapsid (N) protein**. (B)** Total IgG separated by SARS-CoV-2 vaccine (ancestral and BA.5) and variant (XBB1.5 and JN.1) spike (S) antigen and pregnancy status. **(C-F)** Relative abundance of IgG subtypes in pregnant and non-pregnant women as stacked bar plots representing each isotype as a percentage of Total

628 IgG by **(C)** ancestral S, **(D)** BA.5 S, **(E)** XBB.1.5 S, and **(F)** JN.1 S. Data were analyzed by (A)
629 repeated measures two-way ANOVA (B) linear mixed effects regression analysis with
630 Bonferroni post-hoc. (C-F) Isotype proportions were analyzed by Chi-squared analysis with
631 values reported under each corresponding graph. Asterisks indicate $p < 0.05$. Stippled line
632 indicates limit of background (LOB) defined as the $\log_{10}$MFI of a defined negative control.
633

634

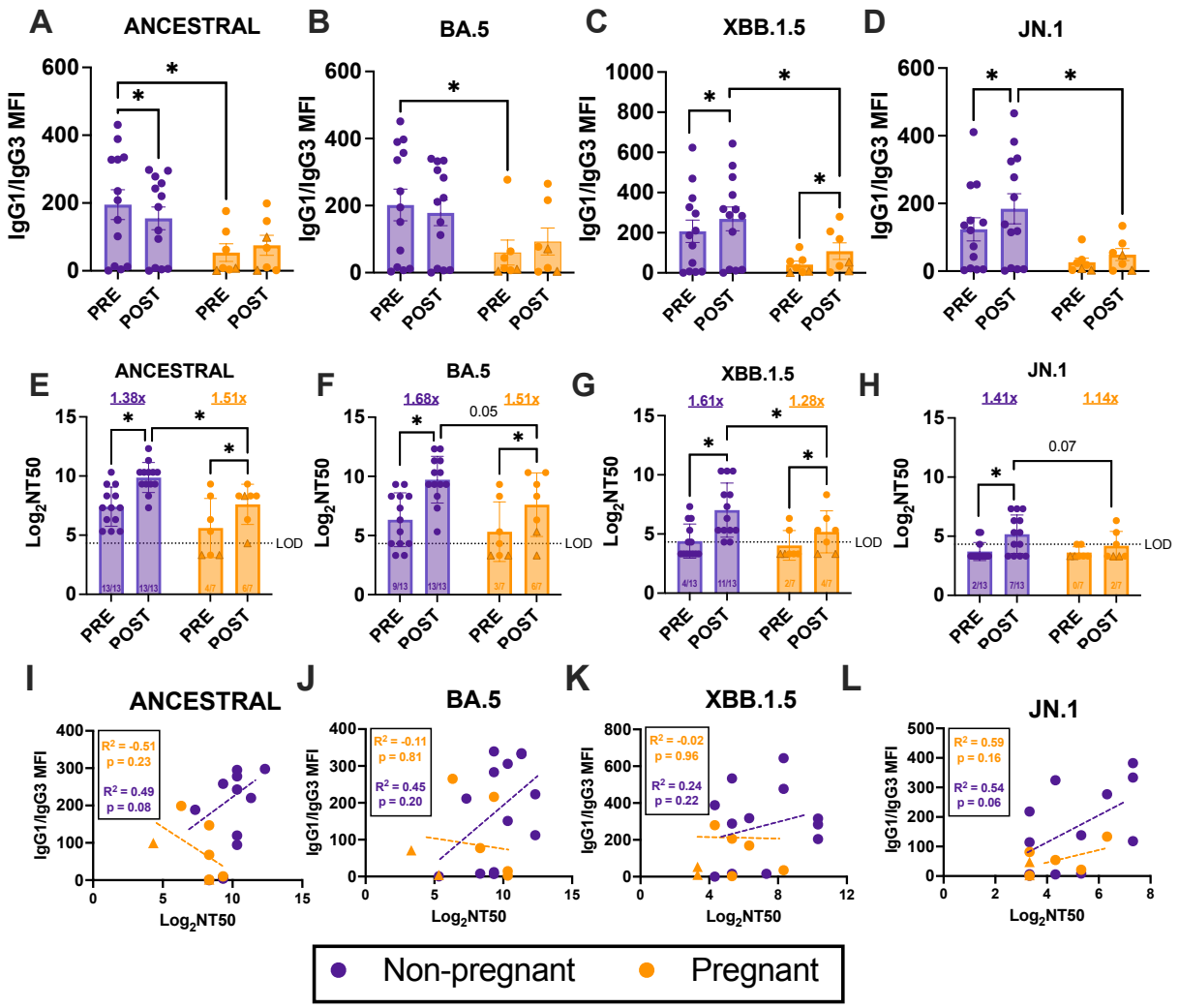

635

636 **Figure 2. Pregnancy alters cross-neutralization of variants of concern.** IgG antibody

637 responses in serum pre and 3-5 weeks post-vaccination were measured by systems

638 serology and reported as mean fluorescence intensity. Pregnant women (n=7) are shown in

639 orange and non-pregnant females (n=13) in purple. Triangles highlight women who received

640 monovalent boosters and circles represent bivalent booster recipients. Bars represent

641 mean MFI across samples with bars indicating standard error of the mean. **(A-E)** Ratio of

642 IgG1:IgG3 antibodies specific to **(A)** ancestral spike (S), **(B)** BA.5 S, **(C)** XBB.1.5 S, and **(D)**

643 JN.1 S. Neutralizing antibody titers reported as Log_2 NT50 against **(E)** ancestral, **(F)** BA.5, **(G)**
644 XBB.1.5, and **(H)** JN.1 viruses. Ratios shown on the x-axis indicate number of women per
645 group/timepoint that are above the limit of detection (LOD) indicated by the stippled line. **(I-**
646 **L)** Pearson correlations between IgG1:IgG3 ratios and neutralizing antibody titers reported
647 as Log_2 NT50 to **(I)** ancestral spike (S), **(J)** BA.5 S, **(K)** XBB.1.5 S, and **(L)** JN.1 S. (A-H) Data
648 were analyzed by repeated measures two-way ANOVA with Bonferroni post-hoc. Asterisks
649 indicate $p < 0.05$. (I-L) Regression lines for each group are shown in dashed lines colored
650 according to cohort. Separate R^2 and p-values are shown for each variant separated by
651 pregnancy status.
652

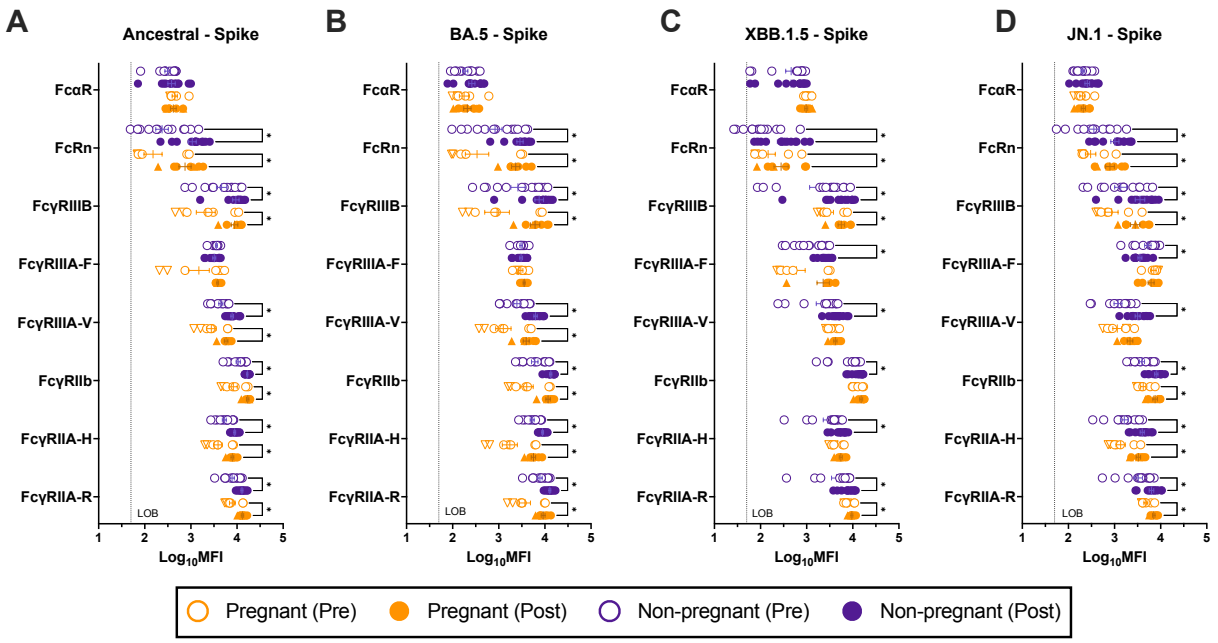

Figure 3. Fc receptor binding is reduced in pregnant women in response to variants of concern. Serum antibody Fc receptor (FcR) binding pre and 3-5 weeks post-vaccination were measured by multiplex Luminex bead assays and reported as $\log_{10}$ mean fluorescence intensity. Pregnant women (n=7) are shown in orange and non-pregnant females (n=13) in purple. Triangles highlight women who received monovalent boosters and circles represent bivalent booster recipients. Horizontal bars indicate mean MFI across samples with bars indicating standard error of the mean. Antibody binging to FcγRIIA-R, FcγRIIA-H, FcγRIIb, FcγRIIIA-V, FcγRIIIA-F, FcγRIIIB, FcRn, and FcαR was determined for **(A)** ancestral spike (S), **(B)** BA.5 S, **(C)** XBB.1.5 S, and **(D)** JN.1 S. Data were analyzed by linear mixed effects regression analysis with Bonferroni post-hoc. Asterisks indicate $p < 0.05$. Stippled line indicates limit of background (LOB) defined as the $\log_{10}$MFI of a defined negative control.

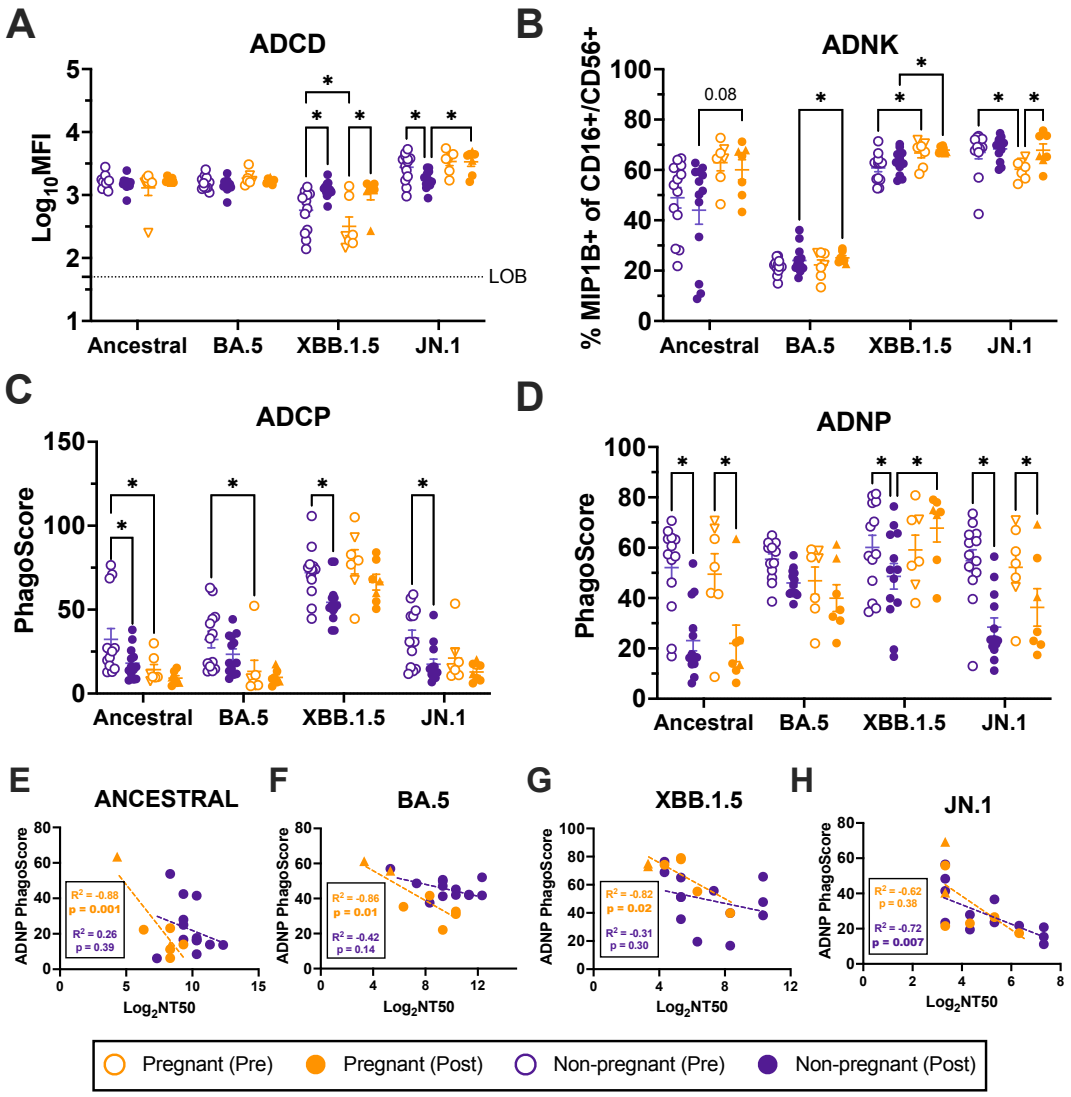

Figure 4. Non-neutralizing and neutralizing antibody functions are negatively correlated among pregnant women. Non-neutralizing antibody functions were measured pre and 3-5 weeks post-vaccination. Pregnant women (n=7) are shown in orange and non-pregnant females (n=13) in purple. Triangles highlight women who received monovalent boosters and circles represent bivalent booster recipients. Horizontal bars indicate mean MFI across samples with bars indicating standard error of the mean. **(A)** antibody dependent complement deposition (ADCD) was measured by assessing antibody binding

674 to C3 protein and is reported as $\log_{10}$ mean fluorescence intensity. Stippled line indicates
675 limit of background (LOB) defined as the $\log_{10}$MFI of a defined negative control. NK cells
676 isolated from donor blood were utilized to assess **(B)** antibody dependent NK cell
677 cytotoxicity (ADNK), or the ability of antigen specific serum antibody to include NK cell
678 cytokine production or degranulation. Data are reported as % MIP1B+ cells of
679 CD16+/CD56+ NK cells. **(C)** THP-1 monocyte cell line was used to measure antibody
680 dependent cellular phagocytosis (ADCP), or the ability of antibody to induce phagocytosis
681 of antigen. **(D)** Neutrophils isolated from donor blood were used to measure antibody
682 dependent neutrophil phagocytosis (ADNP), or the ability of antibody to induce neutrophil
683 phagocytosis of antigen. ADCP and ADNP are reported as a PhagoScore, calculated as (%
684 bead positive monocytes/neutrophils) * (geometric MFI of each cell). **(E-H)** Pearson
685 correlations between post-vaccination neutralizing antibody titers (Log_2NT50) and ADNP
686 PhagoScores for are shown for: **(E)** ancestral, **(F)** BA.5, **(G)** XBB.1.5, and **(H)** JN.1 viruses. (A-
687 E) Data were analyzed by linear mixed effects regression analysis with Bonferroni post-hoc
688 with asterisks indicating $p < 0.05$. (E-H) Separate Pearson correlation R^2 and p-values are
689 shown for each variant separated by pregnancy status, with $p < 0.05$ shown in bolded font.
690 Regression lines for each group are shown in dashed lines colored according to cohort.

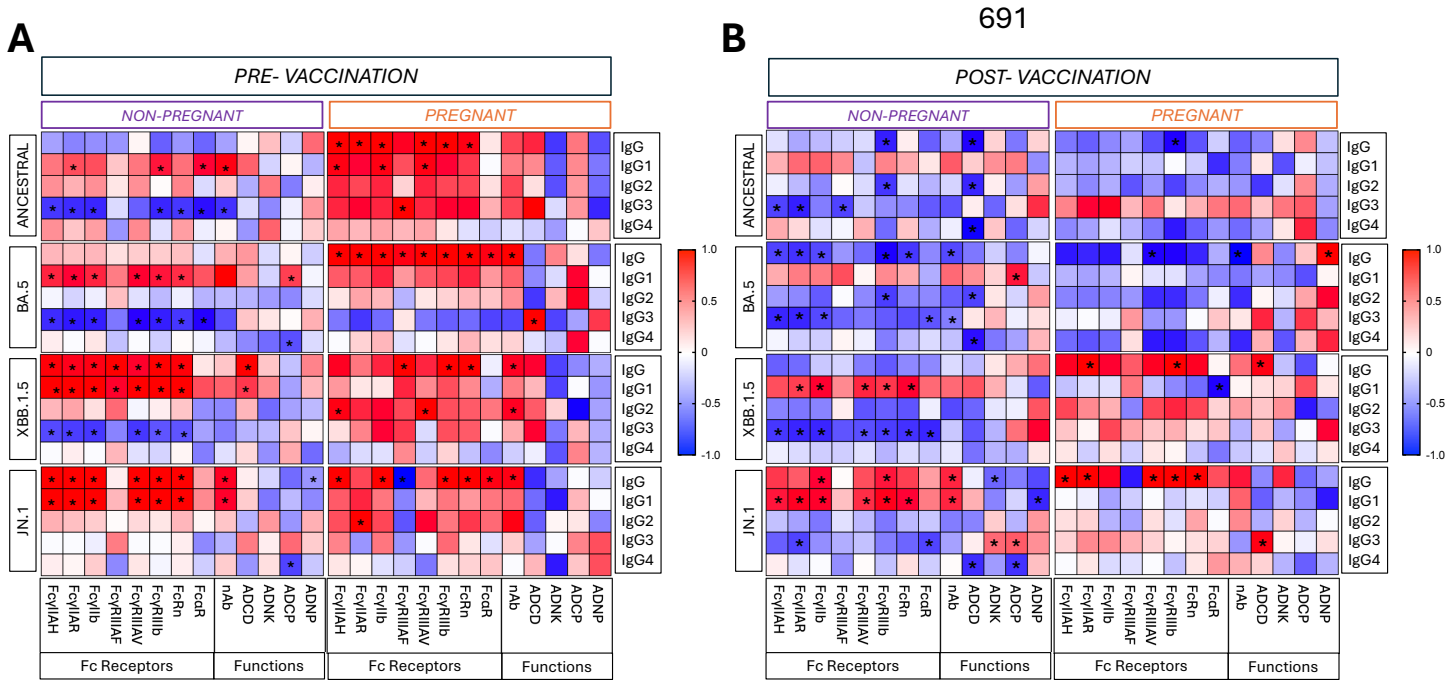

692 **Figure 5. Correlations among IgG subclasses and antibody functional phenotypes**

693 **differ between pregnant and nonpregnant women. (A**) Pre-vaccination and **(B)** post-

694 vaccination systems serology measures including isotype subclasses, FcR binding, non-

695 neutralizing functions, and neutralizing antibody titers were $\log_{10}$ transformed and used for

696 Spearman correlation analyses. Isotypes (y-axis) were correlated with functional measures

697 (x-axis). Analyses were performed by pregnancy status. Asterisks indicate $p < 0.05$. Colors

698 indicate Spearman correlation R value with a positive correlation of 1 indicated by deep red

699 and a negative correlation of 1 indicated by deep blue. Abbreviations defined as followed:

700 ADNP – antibody dependent neutrophil phagocytosis; ADCP – antibody dependent cellular

701 phagocytosis; ADNK – antibody dependent NK cell cytotoxicity; ADCD – antibody

702 dependent complement deposition; NT – neutralizing antibody titer.

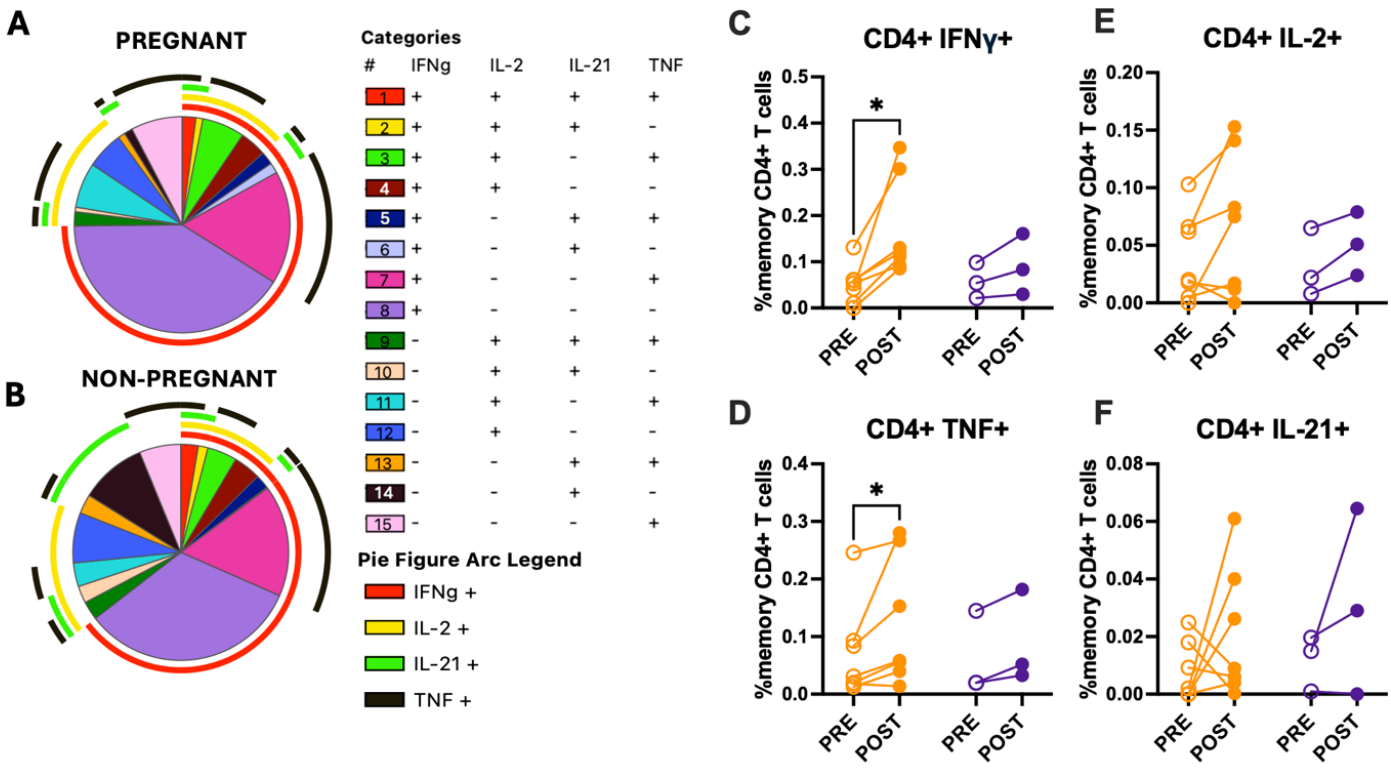

Figure 6. CD4+ T cells have reduced polyfunctionality among pregnant women. Peripheral blood mononuclear cells (PBMCs) were collected pre and 3-5 weeks post-vaccination for flow cytometry analyses. Cytokine-producing, antigen-specific $CD4^+$ T cells for **(A)** pregnant (n=7) and **(B)** non-pregnant (n=3) women represented in pie charts broken down by the 15 cytokine combination categories. Arcs identify portions of the pie that express each specific cytokine**.** Paired dot plots demonstrate the percent of memory $CD4^+$ T cell producing **(C)** IFNγ, **(D)** TNF, **(E)** IL-2, or **(F)** IL-21 following stimulation with ancestral SARS-CoV-2 spike peptide pools pre- and post-vaccination. Data were analyzed by linear mixed effects regression analysis with Bonferroni post-hoc. Asterisks indicate $p < 0.05$.

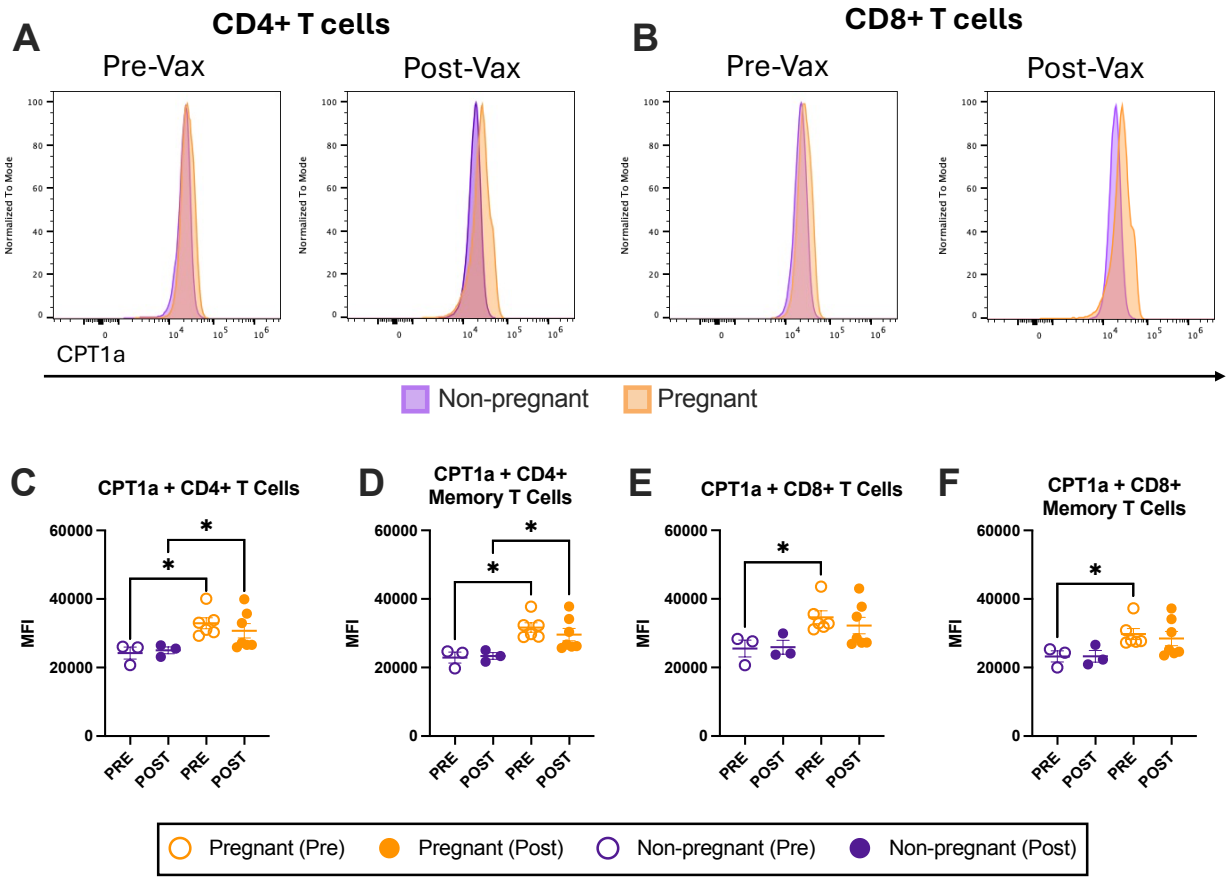

713 **Figure 7. Carnitine palmitoyl transferase 1A (CPT1a) expression in CD4+ and CD8+ T**
714 **cells pre- and post-vaccination is higher in pregnant women.** Peripheral blood
715 mononuclear cells (PBMCs) were collected pre and 3-5 weeks post-vaccination for flow
716 cytometry analyses. Histograms showing CPT1a expression in total **(A)** $CD4^+$ and **(C)** $CD8^+$ T
717 cells from peripheral blood mononuclear cells collected pre- and 3–5 weeks post-
718 vaccination. Pregnant individuals (n=7) are shown in orange and non-pregnant individuals
719 (n=3) in purple. Quantification of mean fluorescence intensity in memory $CD4^+$ **(B)** and
720 memory CD8+ **(D)** T cells are shown for each group pre- and post-vaccination. Horizontal
721 bars indicate mean MFI across samples with bars indicating standard error of the mean.
722 Data were analyzed by linear mixed effects regression analysis with Bonferroni post-hoc.
723 Asterisks indicate $p < 0.05$.

724 **Table 1.**

	Non-Pregnant n = 10	Pregnant n = 7	P-Value
Demographics	Mean ± SD	Mean ± SD	
Age	31.8 ± 3.35	32.9 ±3.18	0.5243734
Vaccine Type	0 0%	2 28.5%	
Monovalent Booster	10 100%	5 71.5%	
Bivalent Booster			
Average Gestational Age (weeks)	-	22.4 ± 11.78	
	N %	**N %**	
Race			
White	6 60.0%	7 100%	
Black	2 20.0%	0 0%	
Asian	2 20.0%	0 0%	
Gestational Age (At Vaccination)	-	1st Trimester (n = 0) 0% 2nd Trimester (n = 6) 85.8% 3rd Trimester (n = 1) 14.2%	

725

726

727 **References**
728

729 1. Engjom, H.M., et al., *Perinatal outcomes after admission with COVID-19 in*
730 *pregnancy: a UK national cohort study.* Nature Communications, 2024. **15**(1): p.
731 3234.
732 2. Brioschi Dos Santos, A.P., et al., *The impact of COVID-19 on maternal death and*
733 *fetal death, a cohort study in Brazil.* PLoS One, 2023. **18**(8): p. e0290343.
734 3. St Clair, L.A., et al., *Reduced control of SARS-CoV-2 infection associates with lower*
735 *mucosal antibody responses in pregnancy.* mSphere, 2024. **9**(3): p. e0081223.
736 4. Strid, P., et al., *Coronavirus Disease 2019 (COVID-19) Severity Among Women of*
737 *Reproductive Age With Symptomatic Laboratory-Confirmed Severe Acute*
738 *Respiratory Syndrome Coronavirus 2 (SARS-CoV-2) Infection by Pregnancy Status-*
739 *United States, 1 January 2020-25 December 2021*. Clin Infect Dis, 2022. **75**(Suppl 2):
740 p. S317-s325.
741 5. Wei, S.Q., et al., *The impact of COVID-19 on pregnancy outcomes: a systematic*
742 *review and meta-analysis*. Cmaj, 2021. **193**(16): p. E540-e548.
743 6. Sessa, R., et al., *SARS-CoV-2 Infection in Pregnancy: Clues and Proof of Adverse*
744 *Outcomes*. Int J Environ Res Public Health, 2023. **20**(3).
745 7. Garcia-Flores, V., et al., *Maternal-fetal immune responses in pregnant women*
746 *infected with SARS-CoV-2*. Nat Commun, 2022. **13**(1): p. 320.
747 8. Verma, S., E.B. Carter, and I.U. Mysorekar, *SARS-CoV2 and pregnancy: An invisible*
748 *enemy?* Am J Reprod Immunol, 2020. **84**(5): p. e13308.
749 9. Doss, J.D., et al., *A prospective cohort study of pregnancy outcomes following*
750 *antepartum infection with SARS-CoV-2*. Pregnancy Hypertens, 2024. **37**: p. 101152.
751 10. Creisher, P.S., et al., *Adverse outcomes in SARS-CoV-2-infected pregnant mice are*
752 *gestational age-dependent and resolve with antiviral treatment*. J Clin Invest, 2023.
753 **133**(20).
754 11. Ciapponi, A., et al., *Safety of COVID-19 vaccines during pregnancy: A systematic*
755 *review and meta-analysis*. Vaccine, 2023. **41**(25): p. 3688-3700.
756 12. Razzaghi, H., et al., *COVID-19 vaccination coverage and intent among women aged*
757 *18-49 years by pregnancy status, United States, April-November 2021*. Vaccine,
758 2022. **40**(32): p. 4554-4563.
759 13. CDC. *COVID-19 Vaccination Coverage, Pregnant Women, United States*. 2025
760 March 19 [cited 2025; Available from: https://www.cdc.gov/covidvaxview/weekly-
761 dashboard/pregnant-persons-vaccination.html.
762 14. Razzaghi H, K.K., Calhoun K, et al., *Influenza, Tdap, and COVID-19 Vaccination*
763 *Coverage and Hesitancy Among Pregnant Women — United States, April 2023*.
764 MMWR Morb Mortal Wkly Rep, 2023.
765 15. Katherine E. Kahn, E.G., Hilda Razzaghi, Tara C. Jatlaoui, Tami H. Skoff, Sascha R.
766 Ellington, Carla L. Black, *Flu, Tdap, and COVID-19 Vaccination Coverage Among*
767 *Pregnant Women – United States, April 2024*. 2024.
768 16. Norman, M., et al., *Neonatal Outcomes After COVID-19 Vaccination in Pregnancy.*
769 Jama, 2024. **331**(5): p. 396-407.

17. CDC. *COVID-19 Vaccination for Women Who Are Pregnant or Breastfeeding*. 2024 September 10, 2024; Available from: https://www.cdc.gov/covid/vaccines/pregnant-or-breastfeeding.html#:~:text=COVID%2D19%20vaccination%20during%20pregnancy,19%20before%20or%20during%20pregnancy.
18. Kumar, D., S. Verma, and I.U. Mysorekar, *COVID-19 and pregnancy: clinical outcomes; mechanisms, and vaccine efficacy*. Transl Res, 2023. **251**: p. 84-95.
19. Casubhoy, I., et al., *A scoping review of global COVID-19 vaccine hesitancy among pregnant persons*. npj Vaccines, 2024. **9**(1): p. 131.
20. Oliver, J., et al., *Drivers of COVID-19 vaccine hesitancy among women of childbearing age in Victoria, Australia: A descriptive qualitative study*. Vaccine: X, 2022. **12**: p. 100240.
21. Hsu, A.L., et al., *Sources of Vaccine Hesitancy: Pregnancy, Infertility, Minority Concerns, and General Skepticism*. Open Forum Infectious Diseases, 2021. **9**(3).
22. Shephard HM, M.S., Nestoridi E, et al. *Inequities in COVID-19 Vaccination Coverage Among Pregnant Persons*. MMWR Morb Mortal Wkly Rep 2023 September 29, 2023.
23. Anderson, M.R., E.J. Hardy, and C.L. Battle, *COVID-19 Vaccine Hesitancy during the Perinatal Period: Understanding Psychological and Cultural Factors to Improve Care and Address Racial/Ethnic Health Inequities*. Womens Health Issues, 2022. **32**(4): p. 317-321.
24. Ramonfaur, D., et al., *Determinants of COVID-19 vaccine hesitancy among pregnant persons*. J Am Pharm Assoc (2003), 2023. **63**(4): p. 1191-1196.
25. Chavan, M., et al., *COVID-19 Vaccination in Pregnancy: The Benefits Outweigh the Risks*. J Obstet Gynaecol Can, 2021. **43**(7): p. 814-816.
26. Kay, A.W. and C.A. Blish, *Immunogenicity and Clinical Efficacy of Influenza Vaccination in Pregnancy*. Front Immunol, 2015. **6**: p. 289.
27. Chayachinda, C., et al., *Immunogenicity and reactogenicity of heterologous COVID-19 vaccination in pregnant women*. Hum Vaccin Immunother, 2023. **19**(2): p. 2228670.
28. Ballivian, J., et al., *Immunogenicity of COVID-19 Vaccines During Pregnancy: A Systematic Review and Comparison of Pregnant Versus Nonpregnant Persons*. Pediatr Infect Dis J, 2025. **44**(2s): p. S27-s31.
29. hemati, Z., et al., *Comparing the immunogenicity of COVID-19 infection and vaccination in pregnant women as measured by anti-S IgG*. BMC Infectious Diseases, 2024. **24**(1): p. 935.
30. Munoz, F.M., et al., *COVID-19 booster vaccination during pregnancy enhances maternal binding and neutralizing antibody responses and transplacental antibody transfer to the newborn*. Vaccine, 2023. **41**(36): p. 5296-5303.
31. Lopez, P.A., et al., *Placental transfer dynamics and durability of maternal COVID-19 vaccine-induced antibodies in infants*. iScience, 2024. **27**(3): p. 109273.
32. Cassidy, A.G., et al., *Assessment of Adverse Reactions, Antibody Patterns, and 12-month Outcomes in the Mother-Infant Dyad After COVID-19 mRNA Vaccination in Pregnancy*. JAMA Netw Open, 2023. **6**(7): p. e2323405.

33. Atyeo, C., et al., *COVID-19 mRNA vaccines drive differential antibody Fc-functional profiles in pregnant, lactating, and nonpregnant women*. Sci Transl Med, 2021. **13**(617): p. eabi8631.
34. Ackerman, M.E., D.H. Barouch, and G. Alter, *Systems serology for evaluation of HIV vaccine trials*. Immunol Rev, 2017. **275**(1): p. 262-270.
35. Fall, A., et al., *The displacement of the SARS-CoV-2 variant Delta with Omicron: An investigation of hospital admissions and upper respiratory viral loads*. EBioMedicine, 2022. **79**: p. 104008.
36. Dhakal, S., et al., *Sex Differences in Lung Imaging and SARS-CoV-2 Antibody Responses in a COVID-19 Golden Syrian Hamster Model*. mBio, 2021. **12**(4): p. e0097421.
37. Dhakal, S., et al., *Reconsideration of Antinucleocapsid IgG Antibody as a Marker of SARS-CoV-2 Infection Postvaccination for Mild COVID-19 Patients*. Open Forum Infect Dis, 2023. **10**(1): p. ofac677.
38. Lee, J.M., et al., *Three doses of COVID-19 mRNA vaccine induce class-switched antibody responses in inflammatory arthritis patients on immunomodulatory therapies*. Front Immunol, 2023. **14**: p. 1266370.
39. Li, M., et al., *Convalescent plasma with a high level of virus-specific antibody effectively neutralizes SARS-CoV-2 variants of concern*. Blood Adv, 2022. **6**(12): p. 3678-3683.
40. Klein, S.L., et al., *Sex, age, and hospitalization drive antibody responses in a COVID-19 convalescent plasma donor population*. J Clin Invest, 2020. **130**(11): p. 6141-6150.
41. Karger, A.B., et al., *The Serological Sciences Network (SeroNet) for COVID-19: Depth and Breadth of Serology Assays and Plans for Assay Harmonization*. mSphere, 2022. **7**(4): p. e0019322.
42. Chung, A.W., et al., *Dissecting Polyclonal Vaccine-Induced Humoral Immunity against HIV Using Systems Serology*. Cell, 2015. **163**(4): p. 988-98.
43. Karsten, C.B., et al., *A versatile high-throughput assay to characterize antibody-mediated neutrophil phagocytosis*. J Immunol Methods, 2019. **471**: p. 46-56.
44. Loos, C., et al., *Systems serology-based comparison of antibody effector functions induced by adjuvanted vaccines to guide vaccine design*. npj Vaccines, 2023. **8**(1): p. 34.
45. Kolde, R., *Pretty Heatmaps*. 2018. p. Implementation of heatmaps that offers more control over dimensions and appearance.
46. Gaeta, A., et al., *Anti-N SARS-CoV-2 assays for evaluation of natural viral infection*. J Immunol Methods, 2023. **518**: p. 113486.
47. Swadźba, J., et al., *High Concentration of Anti-SARS-CoV-2 Antibodies 2 Years after COVID-19 Vaccination Stems Not Only from Boosters but Also from Widespread, Often Unrecognized, Contact with the Virus*. Vaccines (Basel), 2024. **12**(5).
48. Uversky, V.N., et al., *IgG4 Antibodies Induced by Repeated Vaccination May Generate Immune Tolerance to the SARS-CoV-2 Spike Protein*. Vaccines (Basel), 2023. **11**(5).

49. Subramanian, S.V. and A. Kumar, *Increases in COVID-19 are unrelated to levels of vaccination across 68 countries and 2947 counties in the United States*. Eur J Epidemiol, 2021. **36**(12): p. 1237-1240.
50. Chen, W., et al., *The kinetics of IgG subclasses and contributions to neutralizing activity against SARS-CoV-2 wild-type strain and variants in healthy adults immunized with inactivated vaccine*. Immunology, 2022. **167**(2): p. 221-232.
51. Sun, K., et al., *SARS-CoV-2 correlates of protection from infection against variants of concern*. Nature Medicine, 2024. **30**(10): p. 2805-2812.
52. Earle, K.A., et al., *Evidence for antibody as a protective correlate for COVID-19 vaccines*. Vaccine, 2021. **39**(32): p. 4423-4428.
53. Flor, N., et al., *Antibodies to SARS-CoV2 induced by vaccination and infection correlate with protection against the infection*. Vaccine, 2023. **41**(48): p. 7206-7211.
54. Izadi, A. and P. Nordenfelt, *Protective non-neutralizing SARS-CoV-2 monoclonal antibodies*. Trends Immunol, 2024. **45**(8): p. 609-624.
55. Mackin, S.R., et al., *Fc-γR-dependent antibody effector functions are required for vaccine-mediated protection against antigen-shifted variants of SARS-CoV-2*. Nat Microbiol, 2023. **8**(4): p. 569-580.
56. Chandler, T.L., et al., *Protective mechanisms of nonneutralizing antiviral antibodies*. PLoS Pathog, 2023. **19**(10): p. e1011670.
57. Lu, Y., et al., *The rising SARS-CoV-2 JN.1 variant: evolution, infectivity, immune escape, and response strategies*. MedComm (2020), 2024. **5**(8): p. e675.
58. Du, M.R., S.C. Wang, and D.J. Li, *The integrative roles of chemokines at the maternal-fetal interface in early pregnancy*. Cell Mol Immunol, 2014. **11**(5): p. 438-48.
59. Bluman, E.M., et al., *Human natural killer cells produce abundant macrophage inflammatory protein-1 alpha in response to monocyte-derived cytokines*. J Clin Invest, 1996. **97**(12): p. 2722-7.
60. Boudreau, C.M., et al., *Antibody-mediated NK cell activation as a correlate of immunity against influenza infection*. Nature Communications, 2023. **14**(1): p. 5170.
61. Lin, Q., et al., *IFN-γ-dependent NK cell activation is essential to metastasis suppression by engineered Salmonella*. Nature Communications, 2021. **12**(1): p. 2537.
62. Tortorici, M.A., et al., *Persistent immune imprinting occurs after vaccination with the COVID-19 XBB.1.5 mRNA booster in humans*. Immunity, 2024. **57**(4): p. 904-911.e4.
63. Atyeo, C., et al., *Distinct Early Serological Signatures Track with SARS-CoV-2 Survival*. Immunity, 2020. **53**(3): p. 524-532.e4.
64. Sha, Z. and R.W. Compans, *Induction of CD4(+) T-cell-independent immunoglobulin responses by inactivated influenza virus*. J Virol, 2000. **74**(11): p. 4999-5005.
65. Thompson, E.A., et al., *Heterologous versus homologous boosting elicits qualitatively distinct, BA.5-cross-reactive T cells in transplant recipients*. JCI Insight, 2023. **8**(10).
66. Roznik, K., et al., *COVID-19 vaccination induces distinct T-cell responses in pediatric solid organ transplant recipients and immunocompetent children*. NPJ Vaccines, 2024. **9**(1): p. 73.

67. Boyd, A., et al., *Pathogen-Specific T Cell Polyfunctionality Is a Correlate of T Cell Efficacy and Immune Protection*. PLoS One, 2015. **10**(6): p. e0128714.
68. Darrah, P.A., et al., *Multifunctional TH1 cells define a correlate of vaccine-mediated protection against Leishmania major*. Nat Med, 2007. **13**(7): p. 843-50.
69. Rakshit, S., et al., *Polyfunctional CD4 T-cells correlating with neutralising antibody is a hallmark of COVISHIELDTM and COVAXIN® induced immunity in COVID-19 exposed Indians*. npj Vaccines, 2023. **8**(1): p. 134.
70. Li, L., et al., *In-depth analysis of SARS-CoV-2-specific T cells reveals diverse differentiation hierarchies in vaccinated individuals*. JCI Insight, 2022. **7**(7).
71. Peng, S.L., S.J. Szabo, and L.H. Glimcher, *T-bet regulates IgG class switching and pathogenic autoantibody production*. Proc Natl Acad Sci U S A, 2002. **99**(8): p. 5545-50.
72. Alspach, E., D.M. Lussier, and R.D. Schreiber, *Interferon γ and Its Important Roles in Promoting and Inhibiting Spontaneous and Therapeutic Cancer Immunity*. Cold Spring Harb Perspect Biol, 2019. **11**(3).
73. Mohr, E., et al., *IFN-{gamma} produced by CD8 T cells induces T-bet-dependent and -independent class switching in B cells in responses to alum-precipitated protein vaccine*. Proc Natl Acad Sci U S A, 2010. **107**(40): p. 17292-7.
74. Ballesteros-Tato, A., et al., *Interleukin-2 inhibits germinal center formation by limiting T follicular helper cell differentiation*. Immunity, 2012. **36**(5): p. 847-56.
75. Pasparakis, M., et al., *Immune and inflammatory responses in TNF alpha-deficient mice: a critical requirement for TNF alpha in the formation of primary B cell follicles, follicular dendritic cell networks and germinal centers, and in the maturation of the humoral immune response*. Journal of Experimental Medicine, 1996. **184**(4): p. 1397-1411.
76. Elsner, R.A. and M.J. Shlomchik, *Germinal Center and Extrafollicular B Cell Responses in Vaccination, Immunity, and Autoimmunity*. Immunity, 2020. **53**(6): p. 1136-1150.
77. Xiong, J., *Fatty Acid Oxidation in Cell Fate Determination*. Trends Biochem Sci, 2018. **43**(11): p. 854-857.
78. Sewell, C.A., et al., *Scientific, ethical, and legal considerations for the inclusion of pregnant people in clinical trials*. Am J Obstet Gynecol, 2022. **227**(6): p. 805-811.
79. Jenkins, B.J., et al., *Does Altered Cellular Metabolism Underpin the Normal Changes to the Maternal Immune System during Pregnancy?* Immunometabolism, 2021. **3**(4): p. e210031.
80. Atyeo, C.G., et al., *Maternal immune response and placental antibody transfer after COVID-19 vaccination across trimester and platforms*. Nature Communications, 2022. **13**(1): p. 3571.
81. Markov, P.V., et al., *The evolution of SARS-CoV-2*. Nature Reviews Microbiology, 2023. **21**(6): p. 361-379.
82. Chi, W.Y., et al., *COVID-19 vaccine update: vaccine effectiveness, SARS-CoV-2 variants, boosters, adverse effects, and immune correlates of protection*. J Biomed Sci, 2022. **29**(1): p. 82.

83. Huiberts, A.J., et al., *Effectiveness of Omicron XBB.1.5 vaccine against infection with SARS-CoV-2 Omicron XBB and JN.1 variants, prospective cohort study, the Netherlands, October 2023 to January 2024*. Euro Surveill, 2024. **29**(10).
84. Rubin, R., *As COVID-19 Cases Surge, Here's What to Know About JN.1, the Latest SARS-CoV-2 "Variant of Interest"*. Jama, 2024. **331**(5): p. 382-383.
85. CDC. *Staying Up to Date with COVID-19 Vaccines*. 2025 January 7, 2025 [cited 2025 March 25]; Available from: https://www.cdc.gov/covid/vaccines/stay-up-to-date.html.
86. Han, X. and Q. Ye, *The variants of SARS-CoV-2 and the challenges of vaccines*. J Med Virol, 2022. **94**(4): p. 1366-1372.
87. Cobey, S., et al., *Concerns about SARS-CoV-2 evolution should not hold back efforts to expand vaccination*. Nat Rev Immunol, 2021. **21**(5): p. 330-335.
88. Monto, A.S., A.S. Lauring, and E.T. Martin, *SARS-CoV-2 Vaccine Strain Selection: Guidance From Influenza*. J Infect Dis, 2022. **227**(1): p. 4-8.
89. Little D, B.E., Kibitel J, Carrico N, McNitt J. , *Which Comorbidities Increase the Risk of a COVID-19 Breakthrough Infection?. Epic Research*. 2022.
90. Regev-Yochay, G., et al., *Correlates of protection against COVID-19 infection and intensity of symptomatic disease in vaccinated individuals exposed to SARS-CoV-2 in households in Israel (ICoFS): a prospective cohort study*. The Lancet Microbe, 2023. **4**(5): p. e309-e318.
91. Goldblatt, D., et al., *Correlates of protection against SARS-CoV-2 infection and COVID-19 disease*. Immunol Rev, 2022. **310**(1): p. 6-26.
92. Mahrokhian, S.H., et al., *COVID-19 vaccines: Immune correlates and clinical outcomes*. Hum Vaccin Immunother, 2024. **20**(1): p. 2324549.
93. Rice, T.F., B. Holder, and B. Kampmann, *Antibody glycosylation in pregnancy and in newborns: biological roles and implications*. Curr Opin Infect Dis, 2020. **33**(3): p. 225-230.
94. Alter, G., T.H.M. Ottenhoff, and S.A. Joosten, *Antibody glycosylation in inflammation, disease and vaccination*. Semin Immunol, 2018. **39**: p. 102-110.
95. Adhikari, E.H., et al., *Diverging Maternal and Cord Antibody Functions From SARS-CoV-2 Infection and Vaccination in Pregnancy*. J Infect Dis, 2024. **229**(2): p. 462-472.
96. Kent, S.J., et al., *Disentangling the relative importance of T cell responses in COVID-19: leading actors or supporting cast?* Nature Reviews Immunology, 2022. **22**(6): p. 387-397.
97. Cai, F., S. Jin, and G. Chen, *The Effect of Lipid Metabolism on CD4(+) T Cells*. Mediators Inflamm, 2021. **2021**: p. 6634532.
98. Bulygin, A.S., et al., *The role of metabolism on regulatory T cell development and its impact in tumor and transplantation immunity*. Front Immunol, 2022. **13**: p. 1016670.
99. Stracuzzi, M., et al., *Short-lived neutralizing activity against SARS-CoV-2 in newborns of immunized mothers*. Pediatr Allergy Immunol, 2025. **36**(4): p. e70084.
100. Johnston, T.S., et al., *Immunological imprinting shapes the specificity of human antibody responses against SARS-CoV-2 variants*. Immunity, 2024. **57**(4): p. 912-925.e4.

101. Yang, Y.J., et al., *Association of Gestational Age at Coronavirus Disease 2019 (COVID-19) Vaccination, History of Severe Acute Respiratory Syndrome Coronavirus 2 (SARS-CoV-2) Infection, and a Vaccine Booster Dose With Maternal and Umbilical Cord Antibody Levels at Delivery.* Obstetrics & Gynecology, 2022. **139**(3): p. 373-380.